

Efficient Fourier representations of families of Gaussian processes

Philip Greengard*

May 31, 2024

Abstract

We introduce a class of algorithms for constructing Fourier representations of Gaussian processes in 1 dimension that are valid over ranges of hyperparameter values. The scaling and frequencies of the Fourier basis functions are evaluated numerically via generalized quadratures. The representations introduced allow for $O(m^3)$ inference, independent of N , for all hyperparameters in the user-specified range after $O(N + m^2 \log m)$ precomputation where N , the number of data points, is usually significantly larger than m , the number of basis functions. Inference independent of N for various hyperparameters is facilitated by generalized quadratures, and the $O(N + m^2 \log m)$ precomputation is achieved with the non-uniform FFT. Numerical results are provided for Matérn kernels with $\nu \in [3/2, 7/2]$ and lengthscale $\rho \in [0.1, 0.5]$ and squared-exponential kernels with lengthscale $\rho \in [0.1, 0.5]$. The algorithms of this paper generalize mathematically to higher dimensions, though they suffer from the standard curse of dimensionality.

1 Introduction

Gaussian process (GP) regression has become ubiquitous as a statistical tool in many applied sciences including astrophysics, environmental sciences, molecular dynamics, financial economics, and social sciences [2, 5, 8, 14, 15, 16, 26, 37].

In most Gaussian process regression problems a user has observed data $\{(x_i, y_i)\}$ where x_1, \dots, x_N are independent variables that belong to some set $D \subseteq \mathbb{R}^d$ and $y_i \in \mathbb{R}$ are dependent variables. The observed data y_1, \dots, y_N are assumed to be observations of the form

$$y_i = f(x_i) + \epsilon_i \tag{1}$$

where ϵ_i is independent and identically distributed (iid) Gaussian noise, and $f : D \rightarrow \mathbb{R}$ is an unknown function, which is given a Gaussian process prior $f(x) \sim \mathcal{GP}(\mu(x), k(x, x'))$ where μ is a user-specified mean function and k is a covariance function [33].

*Department of Statistics, Columbia University, pg2118@columbia.edu. Research supported by the Alfred P. Sloan Foundation.

The primary computational limitation of GP regression as a practical tool is the cost of the matrix inversion and determinant that appear in the likelihood function of a Gaussian process

$$p(\mathbf{y}) \propto \frac{1}{|\mathbf{K} + \sigma^2 \mathbf{I}|^{1/2}} \exp^{-\frac{1}{2} \mathbf{y}^\top (\mathbf{K} + \sigma^2 \mathbf{I})^{-1} \mathbf{y}}, \quad (2)$$

where \mathbf{K} is the $N \times N$ matrix such that $\mathbf{K}_{i,j} = k(x_i, x_j)$ and σ^2 is the variance of the iid observation noise. For a general symmetric matrix, direct inversion and determinant evaluation both require $O(N^3)$ operations, which for many modern problems is far too costly. A large body of literature has emerged over the last couple of decades on efficient schemes for evaluating these quantities when N is large (i.e. greater than around 10,000). Often, these computational methods rely on taking advantage of the particular structure of covariance matrices [1, 14, 28], approximating the covariance matrix with a low-rank matrix (reduced-rank methods) [19, 31, 36], spectral methods [21, 24, 32], or many more strategies.

In this paper we introduce numerical algorithms for representing a zero-mean Gaussian process f with a translation-invariant covariance kernel k as a random expansion of the form

$$f(x) \sim \sum_{i=1}^m \alpha_i \gamma_i \cos(2\pi \xi_i x) + \beta_i \gamma_i \sin(2\pi \xi_i x), \quad (3)$$

where for $i = 1, \dots, m$ the frequencies $\xi_i \in \mathbb{R}$ are fixed, and α_i and β_i are the iid Gaussians

$$\alpha_i, \beta_i \sim \mathcal{N}(0, 1). \quad (4)$$

The coefficients γ_i of (3) are defined by

$$\gamma_i = \sqrt{2w_i \hat{k}(\xi_i)}, \quad (5)$$

where \hat{k} denotes the Fourier transform of the covariance kernel and $w_i > 0$. The numerical work in constructing expansion (3) involves finding the frequencies ξ_i and the weights w_i such that expansion (3) has an effective covariance kernel that approximates the desired kernel (or family of kernels) to high accuracy. We provide numerical results for constructing an expansion of the form (3) that is valid for all Matérn kernels with $\rho \in [0.1, 0.5]$, and $\nu \in [3/2, 7/2]$. We also include results for approximating (3) with squared-exponential kernels with $\rho \in [0.1, 0.5]$.

There are several advantages to using expansion (3) as a representation of a family of GPs. One computational benefit stems from the so-called weight-space approach to Gaussian process regression (see e.g. [33], [19], [13]) in which the posterior density is defined over the coefficients of a basis function expansion such as (3). Specifically, given data $\{(x_i, y_i)\}$ and a covariance kernel k , weight-space Gaussian process regression is the L^2 -regularized linear regression

$$\begin{aligned} \mathbf{y} &\sim \mathbf{X}\boldsymbol{\beta} + \boldsymbol{\epsilon} \\ \boldsymbol{\epsilon} &\sim \mathcal{N}(0, \sigma^2 \mathbf{I}) \\ \boldsymbol{\beta} &\sim \mathcal{N}(0, \mathbf{I}) \end{aligned} \quad (6)$$

where $\boldsymbol{\beta} \in \mathbb{R}^{2m}$ is the vector of coefficients and \mathbf{X} is the $N \times 2m$ matrix

$$\mathbf{X} = \begin{bmatrix} \gamma_1 \cos(\xi_1 x_1) & \dots & \gamma_m \cos(\xi_m x_1) & \gamma_1 \sin(\xi_1 x_1) & \dots & \gamma_m \sin(\xi_m x_1) \\ \gamma_1 \cos(\xi_1 x_2) & \dots & \gamma_m \cos(\xi_m x_2) & \gamma_1 \sin(\xi_1 x_2) & \dots & \gamma_m \sin(\xi_m x_2) \\ \vdots & & \vdots & \vdots & & \vdots \\ \gamma_1 \cos(\xi_1 x_N) & \dots & \gamma_m \cos(\xi_m x_N) & \gamma_1 \sin(\xi_1 x_N) & \dots & \gamma_m \sin(\xi_m x_N) \end{bmatrix}. \quad (7)$$

The posterior density corresponding to (6) is defined over $2m$ dimensions (assuming σ is fixed) and the posterior mean function is given by

$$\sum_{i=1}^m \bar{\boldsymbol{\beta}}_{1,i} \gamma_i \cos(\xi_i x) + \bar{\boldsymbol{\beta}}_{2,i} \gamma_i \sin(\xi_i x) \quad (8)$$

where $[\bar{\boldsymbol{\beta}}_1 \bar{\boldsymbol{\beta}}_2]^\top$ is the solution to the linear system of equations

$$(\mathbf{X}^\top \mathbf{X} + \sigma^2 \mathbf{I}) \bar{\boldsymbol{\beta}} = \mathbf{X}^\top \mathbf{y}. \quad (9)$$

The equivalence between the solution to (9) and the solution to the so-called function space system in (2) is described in [20].

Representing a GP with Fourier expansion (3) has the advantage that GP regression via linear system (9) can be solved in $O(N + m^3)$ operations. For a general $N \times 2m$ matrix, \mathbf{X} , solving linear system (9) requires $O(Nm^2)$ operations, which can be prohibitively expensive. However, since we use Fourier expansions, the $2m \times 2m$ matrix $\mathbf{X}^\top \mathbf{X}$ can be formed in $O(N + m^2 \log m)$ operations using a non-uniform fast Fourier transform (FFT) [11, 17]. The efficient formation of $\mathbf{X}^\top \mathbf{X}$ reduces the total computational cost of solving the linear system from $O(Nm^2)$ operations to $O(N + m^3)$. In general, m is sufficiently small that m^3 operations is easily affordable on a laptop. Furthermore, for GP problems that involve fitting hyperparameters, the cost of solving linear system (9) is $O(m^3)$ operations for all hyperparameters after a precomputation of $O(N + m^2 \log m)$ operations.

The numerical work in finding ξ_i and w_i of Fourier expansion (3) reduces to constructing a quadrature rule (see, e.g. [27]) for an inverse Fourier transform. Specifically, if k is an integrable translation-invariant covariance kernel with Fourier transform \hat{k} , then k satisfies

$$k(x) = \int_{\mathbb{R}} \hat{k}(\xi) e^{2\pi i \xi x} d\xi. \quad (10)$$

It turns out that expansion (3) can be constructed by evaluating $\xi_i \in \mathbb{R}$ and $w_i \in \mathbb{R}^+$ such that $k(x)$ is well approximated by the sum

$$\sum_{j=1}^n w_j \hat{k}(\xi_j) e^{2\pi i \xi_j x} \quad (11)$$

for a family of covariance kernels where x is in some region of interest.

In this paper, we find ξ_i and w_i with algorithms for constructing generalized Gaussian quadratures. The theory associated with generalized Gaussian quadratures was originally

introduced in 1966 [23] and more recently, efficient numerical algorithms have made constructing generalized Gaussian quadratures practical for many modern problems [7, 27]. The use of such quadratures is now widespread in several environments including in computational physics for the solution of integral equations with singular kernels, and in the numerical solution of certain partial differential equations (e.g. [6, 22, 27]).

Fourier representation (3) is also used in [20] for representing GPs, though in [20] the frequencies ξ_1, \dots, ξ_m are equispaced (and lie on a Cartesian grid in higher dimensions). The primary purpose of that choice of quadrature is its benefits in 2 and 3 dimensions for spatial and spatio-temporal problems. By using equispaced nodes, the weight space matrix of (9) has Toeplitz structure and can be applied in $O(m \log m)$ operations allowing the efficient use of iterative solvers. The dense linear algebra solvers that are used in this paper are impractical in high dimensions since the number of basis functions required for a fixed level of accuracy grows exponentially in dimension.

In one dimension, the generalized quadrature approach of this paper can offer a significant advantage over the equispaced approach, especially for problems that involve fitting hyperparameters. It is common to fit hyperparameters over ranges of values that include kernels that concentrate near zero in the spectral domain (e.g., large lengthscale ρ in Matérn kernel (27)) as well as those that have slow decay at infinity in the spectral domain (e.g., small ν in (27)). Using an equispaced quadrature rule to simultaneously integrate those kernels would require a small grid spacing over a large interval and thus a large number of nodes. Here, we use algorithms for generalized quadratures to construct quadrature rules that simultaneously discretize such families of functions to high accuracy.

The basis function approach of this paper is similar in spirit to several popular basis function approaches including [19, 24, 32]. The methods of this paper, however, have two primary advantages.

- Fourier basis functions are amenable to fast algorithms for solving the linear systems of GP regression. We capitalize on this fact to obtain $O(N + m^3)$ computational complexity for GP regression.
- The Fourier expansions of this paper are valid over families of covariance kernels, whereas other basis function approaches require recomputing basis functions for kernels with different hyperparameter values. As a result, adaptation of hyperparameters is simplified. For all hyperparameter values in the domain of the Fourier expansion, GP regression is performed in $O(m^3)$ operations after a precomputation of $O(N + m^3)$ operations.

There have been a number of kernel approximation methods introduced that, like the methods of this paper, approximate a kernel via quadrature in the Fourier domain of a translation-invariant kernel. For example, the random Fourier features approach of [32] uses a Monte-Carlo integration in Fourier domain and [29] introduces a more general set of quadratures that also rely on random features. Deterministic, higher-order quadrature methods have also been introduced for this purpose. For example, in [10, 35], Gaussian (or Gauss-Legendre) nodes and weights are used for integration in Fourier domain. Such methods can be effective for an individual kernel, but are generally less useful for integrating commonly-used families of spectral densities.

The remainder of this paper is structured as follows. In the following section, we introduce theoretical and numerical tools for representing GPs as Fourier expansions. In Section 3 we describe fast algorithms for GP regression. We provide the numerical results of the algorithms of this paper in Section 4. We conclude with a brief discussion of future directions of research in Section 5.

2 Spectral representation of GPs

Translation invariant (or stationary) covariance kernels are commonly used in practice and include kernel families such as Matérn, squared-exponential, rational quadratic, periodic, and many more [33]. A translation invariant kernel is a function $k(x, y) : \mathbb{R}^d \times \mathbb{R}^d \rightarrow \mathbb{R}$ that can be expressed as a function of $x - y$. In a slight abuse of notation we refer to translation invariant kernels $k(x, y)$ as functions of one variable, $k(x)$ for $x \in \mathbb{R}$.

All of the previously mentioned stationary kernels are also isotropic, that is, they are functions $k(x, y)$ that depend on $\|x - y\|$. For those kernels, $k(x) = k(-x)$, their Fourier transforms are real-valued and symmetric. However, not all symmetric functions are valid covariance kernels. Translation invariant kernels have a particular property— k is a valid kernel if and only if its Fourier transform is non-negatively valued. This property is known as Bochner’s theorem [33].

Clearly an integrable translation-invariant kernel k can be expressed as the inverse Fourier transform

$$k(x) = \int_{-\infty}^{\infty} \hat{k}(\xi) e^{2\pi i \xi x} d\xi, \quad (12)$$

or equivalently, since \hat{k} is even,

$$k(x) = \int_0^{\infty} 2\hat{k}(\xi) \cos(2\pi \xi x) d\xi. \quad (13)$$

A discretized version of integral (13), or an order- n quadrature rule for approximating the integral is a sum of the form

$$k(x) \approx \sum_{j=1}^m 2w_j \hat{k}(\xi_j) \cos(2\pi \xi_j x) =: k'(x), \quad (14)$$

where $\xi_j > 0$ and $w_j > 0$ ¹.

The following theorem demonstrates that any sum of the form (14) corresponds to a basis function representation of a Gaussian process with a covariance kernel that approximates k with the accuracy of discretization (14).

Theorem 1. *Let f be the random expansion defined by*

$$f(x) \sim \sum_{i=1}^m \alpha_i \gamma_i \cos(2\pi \xi_i x) + \beta_i \gamma_i \sin(2\pi \xi_i x), \quad (15)$$

¹The weights w_j need not be positively valued, though throughout this paper, and in general in the literature, w_j are assumed to be positively valued.

where for all $i, j = 1, \dots, m$

$$\alpha_i, \beta_j \sim \mathcal{N}(0, 1) \quad (16)$$

are iid and γ_i are defined by

$$\gamma_i = \sqrt{2w_i \hat{k}(\xi_i)} \quad (17)$$

for some $\xi_i, w_i > 0$. Then f is a Gaussian process distribution with covariance kernel k' defined by the formula

$$k'(x) = \sum_{i=1}^m 2w_i \hat{k}(\xi_i) \cos(2\pi \xi_i x). \quad (18)$$

Proof. Using the independence of the Gaussian coefficients of f , clearly,

$$\begin{aligned} E[f(x)f(y)] &= \sum_{j=1}^m 2w_j \hat{k}(\xi_j) \cos(2\pi \xi_j x) \cos(2\pi \xi_j y) + \sum_{j=1}^m 2w_j \hat{k}(\xi_j) \sin(2\pi \xi_j x) \sin(2\pi \xi_j y) \\ &= \sum_{j=1}^m 2w_j \hat{k}(\xi_j) \left(\cos(2\pi \xi_j x) \cos(2\pi \xi_j y) + \sin(2\pi \xi_j x) \sin(2\pi \xi_j y) \right) \end{aligned} \quad (19)$$

Applying standard trigonometric properties to (19), we obtain

$$E[f(x)f(y)] = \sum_{j=1}^m 2w_j \hat{k}(\xi_j) \cos(2\pi \xi_j (x - y)). \quad (20)$$

□

An immediate consequence of Theorem 1 is that an m -point quadrature rule for the evaluation of the inverse Fourier transform of a covariance kernel provides a weight-space representation of that Gaussian process. Moreover the accuracy of the quadrature rule is exactly the accuracy of the effective covariance kernel. Specifically,

$$\left| \int_0^\infty 2\hat{k}(\xi) \cos(2\pi \xi x) d\xi - \sum_{j=1}^m 2w_j \hat{k}(\xi_j) \cos(2\pi \xi_j x) \right| = |k(x) - k'(x)|. \quad (21)$$

Due to the computational demands of computing with Gaussian processes, practitioners often make tradeoffs between accuracy of some approximate inference algorithm and computational efficiency. In the algorithm of this paper, we use quadrature rules, discussed in subsequent sections, that are equipped with theoretical guarantees on their accuracy. These guarantees on quadrature accuracy translate directly to guarantees on pointwise kernel approximation error due to (21). We now describe the numerical procedure we use for constructing quadrature rules for Gaussian process representation (15).

2.1 Gaussian quadratures for covariance kernels

In the numerical scheme of [7] for constructing generalized Gaussian quadratures, the user inputs functions $\phi_1, \dots, \phi_n : [a, b] \rightarrow \mathbb{R}$ for some $n > 1$ and is returned the nodes $x_1, \dots, x_m \in [a, b]$ and weights $w_1, \dots, w_m \in \mathbb{R}^+$ such that

$$\left| \int_a^b \phi_j(x) dx - \sum_{i=1}^m w_i \phi_j(x_i) \right| < \epsilon \quad (22)$$

for some user-specified $\epsilon > 0$ for all $j = 1, \dots, n$.

In this paper, we are concerned with constructing a particular class of quadrature rules. If f is a Gaussian process defined on $[a, b]$ with covariance kernel k , then we seek to approximate integrals of the form

$$\int_0^\infty 2\hat{k}(\xi) \cos(2\pi\xi t) d\xi \quad (23)$$

for all $t \in [0, b - a]$, which contains $\{|x - y| : x, y \in [a, b]\}$. We therefore use the numerical scheme in [7] to construct quadrature rules for the set of functions

$$\phi_j(\xi) = 2\hat{k}(\xi) \cos(2\pi\xi t_j) \quad (24)$$

for $j = 1, 2, \dots, n$ and $\xi \in [0, \infty)$. Since the integrals in (23) are smooth functions in t , it is sufficient to choose t_1, \dots, t_n as, for example, order- n Chebyshev nodes on $[0, b - a]$ [38], provided that n is sufficiently large. This procedure can be viewed as expanding a smooth function in Chebyshev series where computation is done in ϵ -precision arithmetic. Specifically, suppose that we construct a quadrature rule with nodes $\xi_1, \dots, \xi_m > 0$ and $w_1, \dots, w_m > 0$ such that

$$\left| \int_0^\infty 2\hat{k}(\xi) \cos(2\pi\xi t_j) d\xi - \sum_{i=1}^m 2w_i \hat{k}(\xi_i) \cos(2\pi\xi_i t_j) \right| < \epsilon \quad (25)$$

for some user-specified $\epsilon > 0$ and $j = 1, \dots, n$. Then for sufficiently large n ,

$$\left| \int_0^\infty 2\hat{k}(\xi) \cos(2\pi\xi t) d\xi - \sum_{i=1}^m 2w_i \hat{k}(\xi_i) \cos(2\pi\xi_i t) \right| < \epsilon \quad (26)$$

for all $t \in [0, b - a]$.

Similarly, we can use the same strategy to discretize a family of covariance functions over ranges of hyperparameters, provided that \hat{k} is a smooth function of those hyperparameters. For example, suppose that f is a GP defined on $[-1, 1]$ with a Matérn kernel $k_{\nu, \rho}$ where $k_{\nu, \rho}$ and its Fourier transform $\hat{k}_{\nu, \rho}$ are defined by

$$\begin{aligned} k_{\nu, \rho}(x) &= \frac{2^{1-\nu}}{\Gamma(\nu)} \left(\sqrt{2\nu} \frac{x}{\rho} \right)^\nu K_\nu \left(\sqrt{2\nu} \frac{x}{\rho} \right) \quad \text{and} \\ \hat{k}_{\nu, \rho}(\xi) &:= \int_{\mathbb{R}} \hat{k}(\xi) e^{2\pi i \xi x} d\xi \propto \frac{\Gamma(\nu + \frac{1}{2})}{\Gamma(\nu) \rho^{2\nu}} \left(\frac{2\nu}{\rho^2} \right)^\nu \left(\frac{2\nu}{\rho^2} + 4\pi^2 \xi^2 \right)^{-(\nu+1/2)}, \end{aligned} \quad (27)$$

where $\nu \geq 1/2$, ρ is the lengthscale, and K_ν is the modified Bessel function of the second kind. Now consider the set of covariance kernels k_{ν_i, ρ_j} for $i, j = 1, \dots, p$ where ν_1, \dots, ν_p are the order- p Chebyshev nodes on $[3/2, 7/2]$ and ρ_1, \dots, ρ_p are the order- p Chebyshev nodes defined on $[0.1, 0.5]$. Then \hat{k} is a smooth function of ν, ρ over their domain and we can use [7] to construct quadrature rules for the family of integrals

$$\int_0^\infty 2\hat{k}_{\nu_i, \rho_j}(\xi) \cos(2\pi\xi t_\ell) d\xi \quad (28)$$

for all $i, j \in \{1, \dots, p\}$ and $\ell \in \{1, \dots, n\}$ up to some tolerance ϵ . For large enough p and n , the resulting quadrature rules satisfy

$$\left| \int_0^\infty 2\hat{k}_{\nu, \rho}(\xi) \cos(2\pi\xi t) d\xi - \sum_{i=1}^m 2w_i \hat{k}_{\nu, \rho}(\xi_i) \cos(2\pi\xi_i t) \right| < \epsilon \quad (29)$$

for all $t \in [0, 2]$, $\rho \in [0.1, 0.5]$, $\nu \in [3/2, 7/2]$.

We used the implementation of [34] for this particular computation with $p = 100$ and $n = 200$. The code took 88 seconds to run on a laptop and returned 86 nodes ξ_1, \dots, ξ_{86} and positive weights w_1, \dots, w_{86} . The results of numerical experiments using this quadrature rule are included in Section 4. We also include in Section 4 results of numerical experiments with squared-exponential kernels, k , defined by

$$k(x) = e^{\frac{-x^2}{2\rho^2}}, \quad (30)$$

where ρ is a lengthscale hyperparameter.

We now describe an algorithm for constructing Fourier representations of Gaussian processes for a range of hyperparameter values.

Algorithm 1. *[Construction of Fourier representations]*

1. Set the interval on which the Gaussian process is defined, $[a, b]$, in addition to the intervals where the hyperparameters $\nu \in [\nu_0, \nu_1]$ and $\rho \in [\rho_0, \rho_1]$ are defined. Additionally, set the error tolerance ϵ for the accuracy of the quadrature, or equivalently accuracy of the effective covariance kernel.
2. Construct a quadrature rule over the region of interest using the algorithm of [7]. Specifically, find nodes $\xi_1, \dots, \xi_m \in \mathbb{R}$ and weights $w_1, \dots, w_m \in \mathbb{R}^+$ such that

$$\left| k(x) - \sum_{i=1}^m 2w_i \hat{k}(\xi_i) \cos(2\pi\xi_i x) \right| < \epsilon \quad (31)$$

for all $\nu \in [\nu_0, \nu_1]$, $\rho \in [\rho_0, \rho_1]$, and $x \in [0, b - a]$.

3. Define $f : [a, b] \rightarrow \mathbb{R}$ to be the random expansion

$$f(x) \sim \sum_{i=1}^m \alpha_i \gamma_i \cos(2\pi\xi_i x) + \beta_i \gamma_i \sin(2\pi\xi_i x), \quad (32)$$

where γ_i are defined in (5) and α_i and β_i are iid standard normal Gaussians. Then f is a Gaussian process with effective covariance kernel k' defined by

$$k'(x) = \sum_{i=1}^n 2w_i \hat{k}(\xi_j) \cos(2\pi\xi_j x). \quad (33)$$

3 Regression

Typically, GP regression is used in the following environment. An applied scientist has observed data $\{(x_i, y_i)_{i=1, \dots, N}\}$ where x_i are independent variables that belong to some interval $[a, b] \in \mathbb{R}$ (for 1-dimensional problems) and $y_i \in \mathbb{R}$ are dependent variables. The observed data y_1, \dots, y_N are assumed to be observations of the form

$$y_i = f(x_i) + \epsilon_i, \quad (34)$$

where ϵ_i is iid Gaussian noise and $f : [a, b] \rightarrow \mathbb{R}$ is an unknown function, which is given a Gaussian process prior with covariance function k . Assumptions about k are critical for statistical inference and typically arise from domain expertise or physical knowledge about the data-generating process. There is a large body of literature on the selection of suitable covariance kernels (e.g. [12, 30, 37]). In many applied settings k is not known a priori, but is assumed to belong to some parametric family of functions (e.g. Matérn, squared-exponential, etc.) that depends on hyperparameters that are fit to the data.

The goal of GP regression is to perform statistical inference on the unknown function f at a set of points $\tilde{x} \in [a, b]$ or to understand certain properties of the data-generating process. Inference typically involves evaluating the mean and covariance of the density, conditional on observed data $\mathbf{x}, \mathbf{y} \in \mathbb{R}^N$. The conditional (or posterior) distribution of f at any $\tilde{x} \in \mathbb{R}$ is the Gaussian

$$f(\tilde{x}) | \mathbf{x}, \mathbf{y} \sim \mathcal{N}(\tilde{\mu}, \tilde{\sigma}^2) \quad (35)$$

with

$$\begin{aligned} \tilde{\mu} &= \mathbf{k}(\tilde{x}, \mathbf{x})(\mathbf{K} + \sigma^2 \mathbf{I})^{-1} \mathbf{y}, \\ \tilde{\sigma}^2 &= k(\tilde{x}, \tilde{x}) - \mathbf{k}(\tilde{x}, \mathbf{x})(\mathbf{K} + \sigma^2 \mathbf{I})^{-1} \mathbf{k}(\mathbf{x}, \tilde{x}), \end{aligned} \quad (36)$$

where σ is the standard deviation of ϵ_i (also called the nugget), the matrix \mathbf{K} is the $N \times N$ covariance matrix $\mathbf{K}_{i,j} = k(x_i, x_j)$, the vector $\mathbf{k}(\mathbf{x}, x') \in \mathbb{R}^N$ is the column vector such that $\mathbf{k}(\tilde{x}, \mathbf{x})_i = k(\tilde{x}, x_i)$, and $\mathbf{k}(\mathbf{x}, \tilde{x}) = \mathbf{k}(\tilde{x}, \mathbf{x})^\top$.

Since $\mathbf{K} + \sigma^2 \mathbf{I}$ is an $N \times N$ matrix, direct inversion is computationally intractable for large N . However, the Fourier representations of this paper admit a natural low-rank approximation to \mathbf{K} . Specifically, \mathbf{K} is well-approximated by $\mathbf{X}\mathbf{X}^\top$ where \mathbf{X} is the $N \times 2m$ matrix defined in (7). In particular, $\mathbf{K}_{i,j} = k(x_i, x_j)$ and $\mathbf{X}\mathbf{X}^\top_{i,j}$ is the quadrature rule approximation to $k(x_i, x_j)$ given by

$$\sum_{\ell=1}^m 2\hat{k}(\xi_\ell) w_\ell \cos(2\pi\xi_\ell(x_i - x_j)). \quad (37)$$

Using $\mathbf{X}\mathbf{X}^\top$ as an approximation of \mathbf{K} , the linear systems that appear in $\tilde{\mu}$ and $\tilde{\sigma}^2$,

$$(\mathbf{K} + \sigma^2\mathbf{I})\mathbf{x} = \mathbf{y} \quad \text{and} \quad (\mathbf{K} + \sigma^2\mathbf{I})\mathbf{x} = \mathbf{k}(\mathbf{x}, \tilde{x}), \quad (38)$$

can be approximated in $O(Nm^2)$ operations using standard direct methods. For problems where Nm^2 operations is computationally infeasible, linear systems (38) can be obtained by solving the weight-space systems described in the following section [20].

3.1 Weight-space inference

In the weight-space approach to inference, the posterior density is defined over the coefficients of the basis function expansion – in this paper a Fourier expansion. Specifically, given data $\{(x_i, y_i)\}$ and a covariance kernel k , Gaussian process regression becomes

$$\begin{aligned} \mathbf{y} &\sim \mathbf{X}\boldsymbol{\beta} + \boldsymbol{\epsilon} \\ \boldsymbol{\epsilon} &\sim \mathcal{N}(0, \sigma^2\mathbf{I}) \\ \boldsymbol{\beta} &\sim \mathcal{N}(0, \mathbf{I}), \end{aligned} \quad (39)$$

where $\boldsymbol{\beta} \in \mathbb{R}^{2m}$ is the vector of coefficients and \mathbf{X} is the $N \times 2m$ matrix (7). The posterior density corresponding to (39) is defined over $2m$ dimensions, the components of $\boldsymbol{\beta}$ (or $2m+1$ including the residual standard deviation σ). The conditional distribution of $\boldsymbol{\beta}$ (conditioning on $\sigma, \mathbf{x}, \mathbf{y}$) is Gaussian. Specifically,

$$\boldsymbol{\beta} \mid \sigma, \mathbf{x}, \mathbf{y} \sim \mathcal{N}(\bar{\boldsymbol{\beta}}, (\mathbf{X}^\top\mathbf{X} + \sigma^2\mathbf{I})^{-1}), \quad (40)$$

where $\bar{\boldsymbol{\beta}}$ is the solution to the linear system of equations

$$(\mathbf{X}^\top\mathbf{X} + \sigma^2\mathbf{I})\bar{\boldsymbol{\beta}} = \mathbf{X}^\top\mathbf{y}. \quad (41)$$

The conditional mean $\bar{\boldsymbol{\beta}} \in \mathbb{R}^{2m}$ is the vector of coefficients of the conditional mean function

$$\sum_{i=1}^m \bar{\boldsymbol{\beta}}_{1,i} \cos(2\pi\xi_i x) + \bar{\boldsymbol{\beta}}_{2,i} \sin(2\pi\xi_i x) \quad (42)$$

for all $x \in [a, b]$.

We now describe a numerical implementation of a solver for this system of equations that requires $O(N + m^3)$ operations by taking advantage of the Fourier representation of GPs.

3.2 Numerical Implementation

For a general $N \times 2m$ matrix \mathbf{X} , the computational complexity of the numerical solution of the linear system of equations

$$(\mathbf{X}^\top\mathbf{X} + \sigma^2\mathbf{I})\mathbf{x} = \mathbf{X}^\top\mathbf{y} \quad (43)$$

is $O(Nm^2)$. For GP regression tasks with large amounts of data, $O(Nm^2)$ can be prohibitively expensive. However, for the linear system that appears in the case of Fourier representations, we take advantage of the structure of \mathbf{X} to reduce the linear solve to $O(N + m^3)$

operations. We do this by constructing the $2m \times 2m$ matrix $\mathbf{X}^\top \mathbf{X}$ in $O(N + m^2 \log m)$ operations using a non-uniform fast Fourier transform (FFT) [11, 19] whereas constructing $\mathbf{X}^\top \mathbf{X}$ ordinarily requires $O(Nm^2)$ operations. After constructing $\mathbf{X}^\top \mathbf{X}$, the cost of the linear solve, for all hyperparameters input into Algorithm 1, is $O(m^3)$.

We observe that $\mathbf{X}^\top \mathbf{X}$ can be factorized as

$$\mathbf{X}^\top \mathbf{X} = \mathbf{B}^\top \mathbf{D} \mathbf{X}'^\top \mathbf{X}' \mathbf{D} \mathbf{B}, \quad (44)$$

where \mathbf{X}' is defined by

$$\mathbf{X}' = \begin{bmatrix} e^{2\pi i \xi_1 x_1} & \dots & e^{2\pi i \xi_m x_1} & e^{2\pi i (-\xi_1) x_1} & \dots & e^{2\pi i (-\xi_m) x_1} \\ e^{2\pi i \xi_1 x_2} & \dots & e^{2\pi i \xi_m x_2} & e^{2\pi i (-\xi_1) x_2} & \dots & e^{2\pi i (-\xi_m) x_2} \\ \vdots & & \vdots & \vdots & & \vdots \\ e^{2\pi i \xi_1 x_N} & \dots & e^{2\pi i \xi_m x_N} & e^{2\pi i (-\xi_1) x_N} & \dots & e^{2\pi i (-\xi_m) x_N} \end{bmatrix}, \quad (45)$$

where \mathbf{D} is the diagonal $2m \times 2m$ matrix

$$\mathbf{D} = \begin{bmatrix} \gamma_1 & & & & & \\ & \ddots & & & & \\ & & \gamma_m & & & \\ & & & \gamma_1 & & \\ & & & & \ddots & \\ & & & & & \gamma_m \end{bmatrix}, \quad (46)$$

(see (5) for the definition of γ_i) and \mathbf{B} is $2m \times 2m$ block matrix

$$\mathbf{B} = \begin{bmatrix} \frac{1}{2} \mathbf{I}_m & \frac{1}{2i} \mathbf{I}_m \\ \frac{1}{2} \mathbf{I}_m & -\frac{1}{2i} \mathbf{I}_m \end{bmatrix}, \quad (47)$$

where \mathbf{I}_m denotes the $m \times m$ identity matrix. The matrix $\mathbf{X}'^\top \mathbf{X}'$ is a symmetric matrix where entry p, q is given by

$$(\mathbf{X}'^\top \mathbf{X}')_{p,q} = \sum_{j=1}^N e^{2\pi i x_j (\xi_p + \xi_q)}, \quad (48)$$

for all $p, q \in \{1, \dots, 2m\}$, where we denote $-\xi_p$ with ξ_{m+p} . The sums of (48) can be evaluated with a type 3 non-uniform FFT, a calculation that requires $O(N + m^2 \log m)$ operations. More precisely, we use the type 3 non-uniform FFT of [4] to compute the sums

$$\sum_{j=1}^N e^{2\pi i x_j \omega_\ell}, \quad (49)$$

where $\ell = 1, \dots, 2m^2 + m$ and $\omega_\ell = \xi_p + \xi_q$ for $p, q \in \{1, \dots, 2m\}$ with $q \geq p$. The total cost of evaluating (49) via the non-uniform FFT is $O(N + m^2 \log m)$ operations. A detailed

description of the algorithm and its computational costs can be found in [4]. We also use the non-uniform FFT to compute $\mathbf{X}^T \mathbf{y}$, the right hand side of (43).

Since matrix multiplications of (44) other than $\mathbf{X}^T \mathbf{X}'$ can be applied in $O(m^2)$ operations, the total cost of forming matrix $\mathbf{X}^T \mathbf{X}$ using a non-uniform FFT is $O(N + m^2 \log m)$. Once $\mathbf{X}^T \mathbf{X}$ is formed, the solution to the linear system and determinant calculation can be obtained in $O(m^3)$ operations using standard direct methods. In the following, we provide an algorithm for solving linear system (43) in $O(N + m^3)$ operations.

Algorithm 2. *[GP regression solver]*

1. Use Algorithm 1 to construct nodes ξ_1, \dots, ξ_m and weights w_1, \dots, w_m of a Fourier expansion for a certain covariance kernel or family of kernels.
2. Use the non-uniform FFT to compute the matrix-vector product

$$\mathbf{X}^T \mathbf{y} \tag{50}$$

that appears in the right hand side of (43).

3. Use the non-uniform FFT to compute the sums

$$\sum_{j=1}^N e^{2\pi i x_j \omega_\ell} \tag{51}$$

where $\ell = 1, \dots, 2m^2 + m$ and $\omega_\ell = \xi_p + \xi_q$ for $p, q \in \{1, \dots, 2m\}$ with $q \geq p$.

4. Construct $\mathbf{X}^T \mathbf{X}$ via

$$\mathbf{X}^T \mathbf{X} = \mathbf{B}^T \mathbf{D} \mathbf{X}'^T \mathbf{X}' \mathbf{D} \mathbf{B}, \tag{52}$$

where \mathbf{D} is defined in (46) and \mathbf{B} is defined in (47).

5. Compute the eigendecomposition (or Cholesky factorization) of $\mathbf{X}^T \mathbf{X}$.
6. For computing the posterior mean or variance of GP regression, solve the linear system

$$(\mathbf{X}^T \mathbf{X} + \sigma^2 \mathbf{I}) \boldsymbol{\beta} = \mathbf{X}^T \mathbf{y}. \tag{53}$$

The determinant of the matrix of (53) can be evaluated via the matrix decomposition computed in step 5.

In Table 2 we provide computation times for solving the linear system of equations (43) as well as forming $\mathbf{X}^T \mathbf{X}$ and the matrix vector multiply $\mathbf{X}^T \mathbf{y}$. Additionally, in Figure 4 we plot the total computation times for GP regression for varying numbers of observations.

3.3 Adaptation of hyperparameters

In certain GP problems, the covariance function, k is known a priori. However, in general, k is assumed to belong to a certain parametric family of functions (e.g. Matérn, squared-exponential, etc.) that depends on hyperparameters that are fit to the data. Methods for fitting hyperparameters to data generally involve performing GP regression and solving the linear system of equations (43) and calculating a determinant for many hyperparameter values.

For those problems, the methods of this paper have several advantages:

- Algorithm 1 can be used to generate a Fourier expansion that is valid over the domain of hyperparameters. That expansion depends on hyperparameters by a rescaling of basis functions (or equivalently by rescaling the prior standard deviation of the coefficients).
- Using Algorithm 2, GP regression and determinant evaluation are performed in $O(m^3)$ operations for all hyperparameters after a precomputation of $O(N + m^2 \log m)$ operations. The precomputation involves the application of non-uniform FFTs (steps 2 and 3 of Algorithm 2).
- Since both the observation noise and the priors on regression coefficients are Gaussian, the posterior density in the coefficients β is also Gaussian. As a result efficient numerical methods can be used for evaluating Bayesian posterior moments [18, 19, 25] for certain problems.
- Evaluation of gradients of the likelihood function can be performed in $O(m^2)$ operations after inversion of the posterior covariance matrix (step 5 in Algorithm 2). The component-wise formula for the gradient of the log-likelihood of the posterior density is given by

$$\frac{\partial}{\partial \theta_j} \log(p(\mathbf{y}|\boldsymbol{\theta})) = \frac{1}{2} \mathbf{y}^\top \mathbf{C}^{-1} \frac{\partial \mathbf{C}}{\partial \theta_j} \mathbf{C}^{-1} \mathbf{y} - \frac{1}{2} \text{tr} \left(\mathbf{C}^{-1} \frac{\partial \mathbf{C}}{\partial \theta_j} \right), \quad (54)$$

where $\theta_j \in \mathbb{R}$ is the j -th hyperparameter (see e.g. [33]), and $\mathbf{C} = \mathbf{X}^\top \mathbf{X} + \sigma^2 \mathbf{I} = \mathbf{B}^\top \mathbf{D} \mathbf{X}'^\top \mathbf{X}' \mathbf{D} \mathbf{B} + \sigma^2 \mathbf{I}$ (see (44)). That is, the gradient of the log-likelihood can be evaluated in a time independent of N , the number of data points, after the one-time $O(N + m^2 \log m)$ cost of construction of $\mathbf{X}'^\top \mathbf{X}'$.

4 Numerical Experiments

In this section we demonstrate the performance of the algorithms of this paper on randomly generated data. We implemented Algorithm 1 and Algorithm 2 in Fortran with the GFortran compiler on a 2.6 GHz 6-Core Intel Core i7 MacBook Pro. All examples were run in double precision arithmetic.

We used Algorithm 1 to construct Fourier expansions for the Gaussian processes defined on $[-1, 1]$ with Matérn kernel (see (27)) for all $\nu \in [3/2, 7/2]$ and $\rho \in [0.1, 0.5]$. We also generated quadratures for the squared-exponential kernel (see (30)) with $\rho \in [0.1, 0.5]$ and

two quadrature tolerances, $\epsilon = 10^{-3}, 10^{-5}$ (see Step 2 of Algorithm 1). We chose these kernels due to their widespread use in applications [33]. The Matérn family’s popularity is largely due to its flexibility in representing processes of varying smoothness. In particular, the parameter ν controls smoothness – a Gaussian process with Matérn kernel is $\lfloor \nu \rfloor$ times mean-squared differentiable. Our choice of hyperparameters for the Matérn kernel represents processes with a range of smoothness properties. We used the implementation of [34] for the generalized Gaussian quadrature with Matérn and squared-exponential kernel. For the Matérn kernel, we set $\epsilon = 10^{-5}$ in Algorithm 1. The total run time for generating the quadrature was 88 seconds. The output of the code was 86 total nodes and weights and all weights were positive. For the squared-exponential kernel, we generated two generalized Gaussian quadratures, one with $\epsilon = 10^{-5}$ and one with $\epsilon = 10^{-3}$. These procedure each took 13 seconds and generated 21 and 16 nodes respectively.

These numerical experiments demonstrate that the number of nodes, m , required to discretize the squared-exponential family of kernels is significantly smaller than the m needed for the Matérn family. Although both families need a similar density of nodes near zero to integrate kernels with large timescales ρ (which concentrate near zero in Fourier domain), the Matérn family requires more nodes at high frequencies. This is because Matérn kernels have slower decay in Fourier domain, with decays ranging from fourth to eighth order for $\rho \in [3/2, 7/2]$, whereas squared-exponential kernels have Gaussian decay. Therefore, while the squared-exponential and Matérn quadratures need similar densities of points near zero for accurate integration, the Matérn quadrature needs many more points at large frequencies

Figure 1 is a plot of the locations of the nodes obtained from this procedure. In Table 4 we list those nodes and the corresponding weights. Figure 2 is the corresponding plot for the squared-exponential quadratures and Tables 5 and 6 are the tables of nodes and weights.

In Figure 3 and Table 1, we provide the L^2 error of the effective covariance kernel for various hyperparameter values. The L^2 error of the effective kernel is defined by the formula

$$\left(\int_{-1}^1 \int_{-1}^1 (k'(x, y) - k(x, y))^2 dx dy \right)^{1/2}, \quad (55)$$

where k' denotes the effective covariance kernel and k denotes the true kernel. Integral (55) was computed numerically using a tensor product of Gaussian nodes and weights. The approximate GP regression algorithm of this paper can be viewed as exact GP regression with a kernel that approximates the user-specified kernel. Here, we choose L^2 to measure the accuracy of that approximation. We note that it was shown in [3] that a uniform bound on the pointwise error $|k(x) - k'(x)| < \epsilon$ for all x implies a bound on the l^2 error in the conditional mean (42) at the data points of $N\epsilon/\sigma^2$.

Tables 2 and 3 contain the results of numerical experiments for Gaussian process regression using Algorithms 1 and 2. The data, $\{(x_i, y_i)\}$ was randomly generated on the interval $[-1, 1]$ via

$$y_i = \cos(3e^{x_i}) + \epsilon_i, \quad (56)$$

where

$$\epsilon_i \sim \mathcal{N}(0, 0.5). \quad (57)$$

The x_i were generated uniformly at random on $[-1, 1]$ and we note that the performance of the algorithm is independent of locations of data points. The nodes and weights of the Fourier expansions used are given by Table 4. We used Algorithm 2 to compute the conditional mean and covariance and report timings in Tables 2 and 3 where N denotes the number of data points, ν denotes the smoothness hyperparameters of the Matérn kernel, and ρ denotes the lengthscale. We used a residual variance, $\sigma^2 = 1$ and note that the performance of the algorithm is independent of this parameter. The L^2 error of the effective covariance kernel (see (55)) is provided in the column “ L^2 error”. We include timings for solving the regression problem via Algorithm 2. In column “ t_{form} (s)” we provide the total time for formation of the matrix $\mathbf{X}^T \mathbf{X}$ and the matrix vector multiply $\mathbf{X}^T \mathbf{y}$. The column “ t_{solve} (s)” denotes the remaining time in the regression solution, which involves inversion of $(\mathbf{X}^T \mathbf{X} + \sigma^2 \mathbf{I})$. The total time is provided in column “ t_{total} (s).” The primary purpose of Tables 2 and 3 is to demonstrate the scaling of compute times for N varying from 10^5 to 10^8 . These timings are independent of the choice of hyperparameters and thus hyperparameters for these experiments were arbitrarily chosen.

The numerical experiments in this section illustrate the two primary advantages of the algorithms of this paper. First, in Table 1 and in Figure 3, we show that generalized quadratures are able to approximate kernels (Matérn and squared-exponential) over ranges of hyperparameters to high accuracy. Second, in Tables 2, 3 and Figure 4, we demonstrate that the solution to the GP linear system can be efficiently computed with fast algorithms. Since m is significantly smaller than N , nearly all compute time in the linear solve is in the $O(N + m^2 \log m)$ precomputation consisting of two non-uniform FFTs for forming $\mathbf{X}^T \mathbf{X}$ and $\mathbf{X}^T \mathbf{y}$. Furthermore, after precomputation the cost of all linear solves is $O(m^3)$. We report timings in column t_{solve} in Tables 2 and 3.

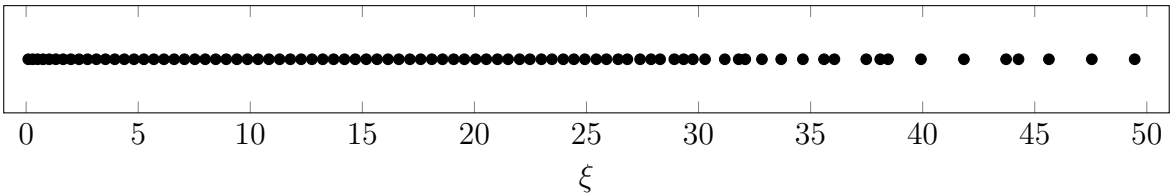


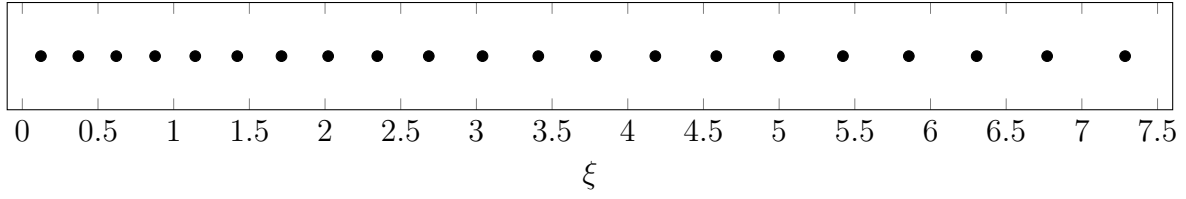
Figure 1: *Location of the 86 nodes for GPs defined on $[-1, 1]$ with Matérn kernels with $\nu \in [1.5, 3.5]$, and $\rho \in [0.1, 0.5]$.*

5 Generalizations and Conclusions

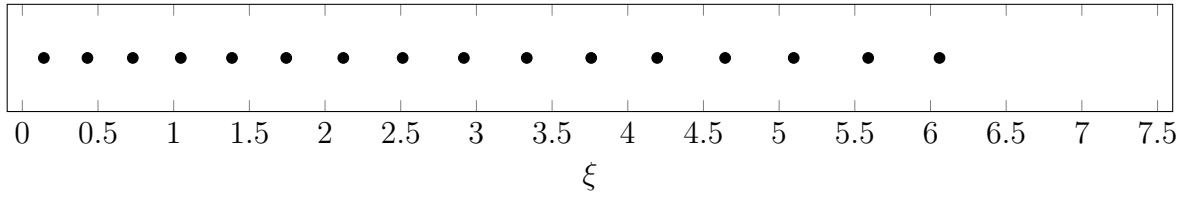
In this paper we introduce algorithms for representing and computing with Gaussian processes in 1-dimension. In Algorithm 1, we describe a numerical scheme for representing families of Gaussian processes as Fourier expansions of the form

$$f(x) \sim \sum_{i=1}^m \alpha_i \gamma_i \cos(2\pi \xi_i x) + \beta_i \gamma_i \sin(2\pi \xi_i x), \quad (58)$$

where for $i = 1, \dots, m$, the frequencies $\xi_i \in \mathbb{R}$ are fixed, $\gamma_i \in \mathbb{R}$, and α_i, β_i are iid standard normal Gaussians. These expansions are constructed in such a way that they are valid over



(a) $\epsilon = 10^{-5}$



(b) $\epsilon = 10^{-3}$

Figure 2: Location of the nodes for GPs defined on $[-1, 1]$ with squared-exponential kernels with $\rho \in [0.1, 0.5]$. Both sets of nodes were generated with Algorithm 1 with different error tolerance ϵ .

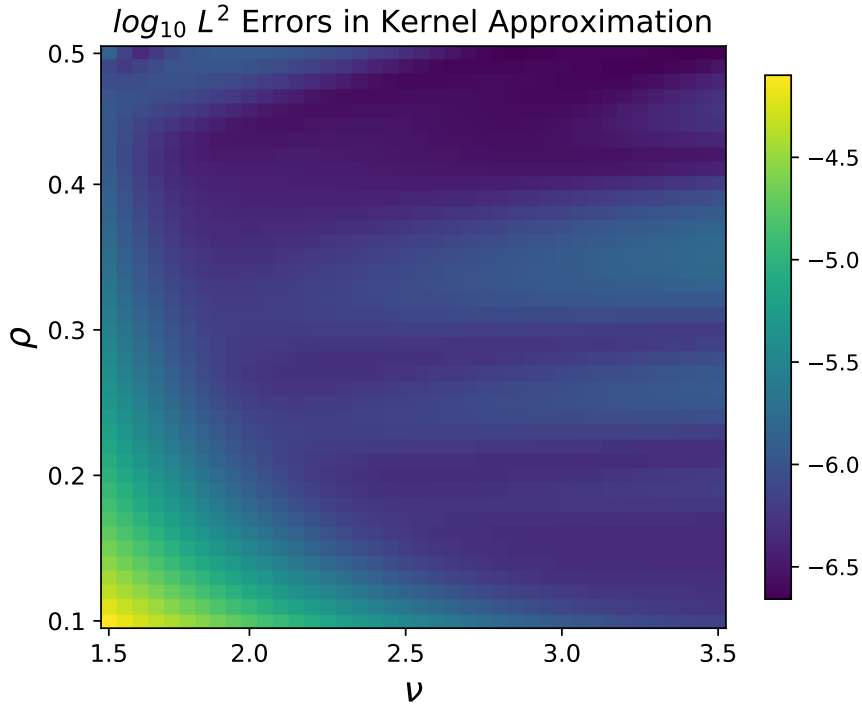


Figure 3: $\log_{10} L^2$ errors in the effective covariance kernel for Matérn kernels. Specifically, we plot $\log_{10} \|k_{\nu,\rho} - k'_{\nu,\rho}\|_2$ for various ν, ρ , where $k'_{\nu,\rho}$ denotes the effective kernel and $k_{\nu,\rho}$ the exact kernel.

ρ	L^2 error	ρ	L^2 error
0.10	0.943×10^{-5}	0.10	0.657×10^{-3}
0.12	0.832×10^{-5}	0.12	0.646×10^{-3}
0.14	0.847×10^{-5}	0.14	0.690×10^{-3}
0.16	0.870×10^{-5}	0.16	0.738×10^{-3}
0.18	0.872×10^{-5}	0.18	0.780×10^{-3}
0.21	0.855×10^{-5}	0.21	0.810×10^{-3}
0.23	0.827×10^{-5}	0.23	0.839×10^{-3}
0.25	0.788×10^{-5}	0.25	0.856×10^{-3}
0.27	0.732×10^{-5}	0.27	0.852×10^{-3}
0.29	0.664×10^{-5}	0.29	0.834×10^{-3}
0.31	0.593×10^{-5}	0.31	0.823×10^{-3}
0.33	0.537×10^{-5}	0.33	0.833×10^{-3}
0.35	0.495×10^{-5}	0.35	0.855×10^{-3}
0.37	0.458×10^{-5}	0.37	0.872×10^{-3}
0.39	0.421×10^{-5}	0.39	0.878×10^{-3}
0.42	0.388×10^{-5}	0.42	0.876×10^{-3}
0.44	0.361×10^{-5}	0.44	0.872×10^{-3}
0.46	0.339×10^{-5}	0.46	0.861×10^{-3}
0.48	0.323×10^{-5}	0.48	0.834×10^{-3}
0.50	0.306×10^{-5}	0.50	0.805×10^{-3}

(a) $\epsilon = 10^{-5}$ (b) $\epsilon = 10^{-3}$

Table 1: Accuracy of Fourier representation (3) for squared-exponential kernels with length-scales $\rho \in [0.1, 0.5]$ and two error tolerances, ϵ . The nodes and weights used are reported in Table 5 and Table 6.

N	ν	ρ	L^2 error	t_{form} (s)	t_{solve} (s)	t_{total} (s)
10^5	3.0	0.1	0.113×10^{-5}	0.03	0.004	0.035
10^6	2.0	0.5	0.118×10^{-4}	0.11	0.005	0.12
10^7	1.5	0.1	0.780×10^{-4}	1.1	0.004	1.1
10^8	3.5	0.3	0.630×10^{-6}	12.0	0.005	12.0

Table 2: Computation times and accuracy for regression with Matérn kernels with $\nu \in [0.5, 3.5]$, and $\rho \in [0.1, 0.5]$. The nodes and weights used are reported in Table 4.

families of covariance kernels. Representing a GP as expansion (58), allows the use of Algorithm 2 to perform GP regression in $O(m^3)$ operations after $O(N+m^2 \log m)$ precomputation where N is the number of data points and m the size of the expansion.

While this paper is focused on GPs in 1-dimensions, much of the theory and numerical machinery extends naturally to higher dimensions. In particular, for GPs over \mathbb{R}^d , one generalization of the 1-dimensional Fourier expansion is the tensor-product expansion of the

N	ρ	L^2 error	t_{form} (s)	t_{solve} (s)	t_{total} (s)
10^5	0.50	0.306×10^{-5}	0.02	0.1×10^{-3}	0.02
10^6	0.20	0.861×10^{-5}	0.09	0.1×10^{-3}	0.10
10^7	0.25	0.782×10^{-5}	1.08	0.1×10^{-3}	1.08
10^8	0.10	0.943×10^{-5}	13.1	0.2×10^{-3}	13.1

(a) Squared-exponential kernel, $\epsilon = 10^{-5}$

N	ρ	L^2 error	t_{form} (s)	t_{solve} (s)	t_{total} (s)
10^5	0.50	0.805×10^{-3}	0.02	0.5×10^{-4}	0.02
10^6	0.20	0.803×10^{-3}	0.10	0.7×10^{-4}	0.10
10^7	0.25	0.857×10^{-3}	1.04	0.6×10^{-4}	1.04
10^8	0.10	0.657×10^{-3}	12.3	0.7×10^{-4}	12.3

(b) Squared-exponential kernel, $\epsilon = 10^{-3}$

Table 3: Computation times and accuracy for regression with squared-exponential kernel with $\rho \in [0.1, 0.5]$. The nodes and weights used are reported in Table 5 and Table 6.

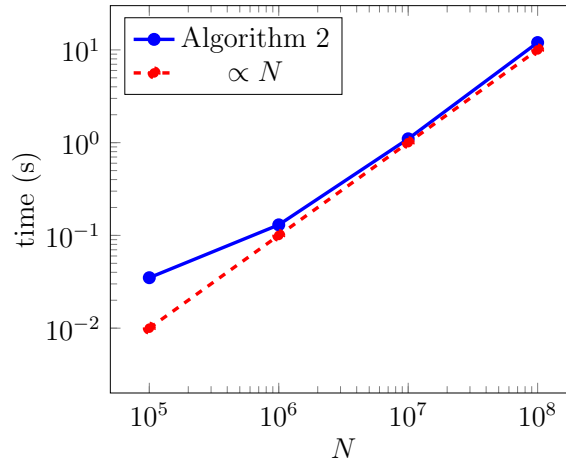


Figure 4: Scaling times for evaluation of conditional mean for varying amounts of data with Matérn kernel. We include a plot proportional to N for comparison.

form

$$f(\mathbf{x}) \sim \sum_{\mathbf{j} \in \{1, \dots, m\}^d} \alpha_{\mathbf{j}} e^{i2\pi \langle \boldsymbol{\xi}_{\mathbf{j}}, \mathbf{x} \rangle}, \quad (59)$$

where $\mathbf{x} \in \mathbb{R}^d$, $\boldsymbol{\xi}_{\mathbf{j}} = (\xi_{j_1}, \xi_{j_2}, \dots, \xi_{j_d})$ where ξ_1, \dots, ξ_m are equispaced real-valued frequencies. This representation of Gaussian process distributions was used in [20] for efficient GP regression in 1, 2, and 3 dimensions. Accompanying error analysis can be found in [3]. As in the 1-dimensional case, the weight-space linear system corresponding to (59) contains structure in d dimensions that is amenable to fast algorithms. In particular, the matrix of the weight-space linear system has d -dimensional Toeplitz structure and can be applied efficiently using the non-uniform FFT, facilitating the use of iterative methods.

We plan to address the higher dimensional extension of the tools of this paper in subsequent publications.

A Detailed results of generalized quadrature

In this section we include tables of quadrature nodes and weights generated by Algorithm 1.

i	nodes	weights	i	nodes	weights
1	0.0960748783232733	0.1933002284075283	44	18.5783668916359304	0.4901095181946152
2	0.2949311558758212	0.2064005047360611	45	19.0739289334232396	0.4936700008508603
3	0.5121811831688609	0.2293690006634405	46	19.5535187961381212	0.4806551264127251
4	0.7553750530381257	0.2574584689846101	47	20.0540157049340202	0.4919980518793062
5	1.0272554775524241	0.2860863008101612	48	20.5303087220011804	0.4886725084331118
6	1.3267469591800769	0.3123806483750251	49	21.0308285956013101	0.4985884540483315
7	1.6509109783729810	0.3353906370922179	50	21.5033438976054896	0.4525339724563319
8	1.9964656597608781	0.3552203181130367	51	22.0147025165826093	0.5300911113825829
9	2.3604331716760738	0.3722929241325456	52	22.4786227659423616	0.4703295964417554
10	2.7402749478447399	0.3870336516793261	53	22.9890428278831500	0.5031381396430530
11	3.1338448880682450	0.3998022537083804	54	23.4620311240316504	0.4385610519729455
12	3.5393213277133500	0.4108896687408796	55	23.9659051179655798	0.5529348248583776
13	3.9551382871240710	0.4205230182176792	56	24.4374955606510014	0.4879736648158969
14	4.3799500415428971	0.4289035535544789	57	24.9268582817982995	0.4320150910275336
15	4.8125843418627330	0.4361897874230700	58	25.4355862458376691	0.5030088994396542
16	5.2520252807076444	0.4425587482527165	59	25.8908822711706499	0.4986129817647325
17	5.6973962780821781	0.4480785412063698	60	26.4135765170375585	0.5698981287926346
18	6.1479398698978196	0.4528922343761104	61	26.8244665781450813	0.3580010222446956
19	6.6029703189280022	0.4571127652712647	62	27.3929596371526216	0.4477770521368305
20	7.0619657471053916	0.4607536593597344	63	27.8810764015625807	0.6306236380217451
21	7.5244050646589304	0.4640030341808996	64	28.2872085273741511	0.5684848926018280
22	7.9898781249339503	0.4668744890692324	65	28.9186103516193818	0.1661641302432533
23	8.4580188390522402	0.4693377032983527	66	29.3361902609053793	0.7145700506865926
24	8.9284697412154603	0.4715695985713800	67	29.7475402852299098	0.3653264402765759
25	9.4010606000280621	0.4735626358176499	68	30.2919596593750207	0.7987670620900847
26	9.8755021184860947	0.4753261760015748	69	31.1707837877708087	0.6496969625503436
27	10.3515866576509996	0.4768203234940871	70	31.7921709344750916	0.6374198048803309
28	10.8290813405759305	0.4782250403991462	71	32.0844373549515112	0.4525776393523478
29	11.3078856905533307	0.4795013762603529	72	32.8290834819148998	0.5792967675329964
30	11.7878547186769005	0.4806019700535451	73	33.6870452221527970	1.2316989151794200
31	12.2690444362196605	0.4816049378992831	74	34.6556177080743311	0.6653181217090052
32	12.7507923286660407	0.4826033499503408	75	35.5973697159031417	0.7979748203948971
33	13.2340308273640499	0.4830779751411056	76	36.0608079398967192	0.9871538295211217
34	13.7168180215943405	0.4845298908539934	77	37.4828497993489194	1.1429690155529550
35	14.2023546685620694	0.4833485049199899	78	38.1056387575873927	0.3983778654241495
36	14.6852339737999902	0.4872979567198063	79	38.4560335475650206	0.7492963615598504
37	15.1736671929864606	0.4828723127156595	80	39.9230354160448471	1.7911442981045280
38	15.6561205601530808	0.4883987918117061	81	41.8408663755605872	1.9661520413352620
39	16.1465532564475396	0.4852092322682524	82	43.7213283268615385	1.6715931870761731
40	16.6287678133340897	0.4863731168868852	83	44.2767860363890975	0.2685526601061519
41	17.1217168205720291	0.4871456130687457	84	45.6320859437675992	1.7725506245674350
42	17.6027784484422583	0.4894715943022971	85	47.5466594857420191	1.9715488370126710
43	18.0975219052295202	0.4843933188273860	86	49.4591701554423580	1.5256479816263220

Table 4: *Nodes and weights for GPs defined on $[-1, 1]$ with Matérn kernels with $\nu \in [0.5, 3.5]$, $\rho \in [0.1, 0.5]$ and generalized quadrature error tolerance $\epsilon = 10^{-5}$*

i	nodes	weights
1	0.1229445208158333	0.2460787859722326
2	0.3699809596646247	0.2483834500933746
3	0.6205086829190636	0.2530883303134549
4	0.8770552409688902	0.2604997558962125
5	1.1425176151727869	0.2709680345476000
6	1.4200169312069510	0.2844795049982405
7	1.7121859512103039	0.3000950603476956
8	2.0204572753950010	0.3164711614602873
9	2.3450325050947400	0.3326020197065039
10	2.6853624988811311	0.3478765986892886
11	3.0404027813093690	0.3619772453611054
12	3.4089356692419108	0.3748597265560644
13	3.7897759561613382	0.3866892173786112
14	4.1819675933484106	0.3975832074366130
15	4.5848345162589501	0.4080437319776904
16	4.9982272332198843	0.4187013160108272
17	5.4216263344213846	0.4286803282747237
18	5.8568375371290067	0.4407898239564511
19	6.3049123731014509	0.4532465428424199
20	6.7704615862559896	0.4793970577067649
21	7.2856984407800462	0.5955092328616340

Table 5: *Nodes and weights for GPs defined on $[-1, 1]$ with squared-exponential kernels with $\rho \in [0.1, 0.5]$ and generalized quadrature error tolerance $\epsilon = 10^{-5}$*

i	nodes	weights
1	0.1422798837388160	0.2849869860136982
2	0.4303383428161451	0.2928359950804127
3	0.7298461801991711	0.3067700728299949
4	1.0470392453484560	0.3273066745906839
5	1.3851554070607901	0.3487384660693318
6	1.7436383837560350	0.3683279469348825
7	2.1204551041309121	0.3845946863247884
8	2.5128009567183280	0.3990369748481500
9	2.9171012161369898	0.4110929506127443
10	3.3326272282803751	0.4225819367888854
11	3.7585126968767120	0.4287907919621072
12	4.1943700876820937	0.4446683446440617
13	4.6430513969235117	0.4594237430500937
14	5.0962967069840737	0.4282067825430210
15	5.5883652398864117	0.5632442756521038
16	6.0596680913512913	0.4616691765322060

Table 6: *Nodes and weights for GPs defined on $[-1, 1]$ with squared-exponential kernels with $\rho \in [0.1, 0.5]$ and generalized quadrature error tolerance $\epsilon = 10^{-3}$*

References

- [1] S. Ambikasaran, D. Foreman-Mackey, L. Greengard, D. W. Hogg, and M. O’Neil. Fast Direct Methods for Gaussian Processes. *IEEE Trans. Pattern Anal. Mach. Intell.*,

- 38(2):252–265, 2016.
- [2] S. Banerjee, A. E. Gelfand, A. O. Finley, and H. Sang. Gaussian predictive process models for large spatial data sets. *Royal Statistical Society*, 70(4):825–848, 2008.
- [3] A. Barnett, P. Greengard, and M. Rachh. Uniform approximation of common gaussian process kernels using equispaced fourier grids. *Applied and Computational Harmonic Analysis*, 71:101640, 2024.
- [4] A. H. Barnett, J. Magland, and L. af Klinteberg. A parallel nonuniform fast fourier transform library based on an “exponential of semicircle” kernel. *SIAM Journal on Scientific Computing*, 41(5):C479–C504, 2019.
- [5] A. P. Bartók, M. C. Payne, R. Kondor, and G. Csányi. Gaussian approximation potentials: The accuracy of quantum mechanics, without the electrons. *Phys. Rev. Lett.*, 104:136403, Apr 2010.
- [6] J. Bremer and Z. Gimbutas. A nyström method for weakly singular integral operators on surfaces. *Journal of Computational Physics*, 231(14):4885–4903, 2012.
- [7] J. Bremer, Z. Gimbutas, and V. Rokhlin. A nonlinear optimization procedure for generalized gaussian quadratures. *SIAM Journal on Scientific Computing*, 32(4):1761–1788, 2010.
- [8] N. Cressie. *Statistics for Spatial Data, Revised Edition*. Wiley-Interscience, Hoboken, NJ, 2015.
- [9] G. Dahlquist and A. Bjork. *Numerical Methods*. Dover, Mineola, NY, 1974.
- [10] T. Dao, C. D. Sa, and C. Ré. Gaussian quadrature for kernel features. In *Proceedings of the 31st International Conference on Neural Information Processing Systems, NIPS’17*, page 6109–6119, Red Hook, NY, USA, 2017. Curran Associates Inc.
- [11] A. Dutt and V. Rokhlin. Fast fourier transforms for nonequispaced data. *SIAM Journal on Scientific Computing*, 14(6):1368–1393, 1993.
- [12] D. Duvenaud. *Automatic Model Construction with Gaussian Processes*. PhD thesis, Computational and Biological Learning Laboratory, University of Cambridge, 2014.
- [13] S. Filip, A. Javeed, and L. N. Trefethen. Smooth Random Functions, Random ODEs, and Gaussian Processes. *SIAM Review*, 61(1):185–205, 2019.
- [14] D. Foreman-Mackey, E. Agol, S. Ambikasaran, and R. Angus. Fast and Scalable Gaussian Process Modeling with Applications to Astronomical Time Series. *The Astronomical Journal*, 154(6), 2017.
- [15] A. Gelman, J. B. Carlin, H. S. Stern, D. B. Dunson, A. Vehtari, and D. B. Rubin. *Bayesian Data Analysis*. Chapman and Hall/CRC, New York, NY, 3rd edition, 2013.

- [16] J. Gonzalez, E. Lezmi, T. Roncalli, and J. Xu. Financial Applications of Gaussian Processes and Bayesian Optimization. *arXiv*, q-fin/1903.04841, 2019.
- [17] L. Greengard and J.-Y. Lee. Accelerating the nonuniform fast fourier transform. *SIAM Review*, 46(3):443–454, 2004.
- [18] P. Greengard, A. Gelman, and A. Vehtari. A Fast Regression via SVD and Marginalization. *Computational Statistics*, 2021.
- [19] P. Greengard and M. O’Neil. Efficient reduced-rank methods for Gaussian processes with eigenfunction expansions. *Statistics and Computing*, 32(5):94, 2022.
- [20] P. Greengard, M. Rachh, and A. Barnett. Equispaced Fourier representations for efficient Gaussian process regression from a billion data points. *arXiv*, stat.CO/2210.10210, 2022.
- [21] J. Hensman, N. Durrande, and A. Solin. Variational fourier features for gaussian processes. *J. Mach. Learn. Res.*, 18(1):5537–5588, 2017.
- [22] J. G. Hoskins, V. Rokhlin, and K. Serkh. On the numerical solution of elliptic partial differential equations on polygonal domains. *SIAM Journal on Scientific Computing*, 41(4):A2552–A2578, 2019.
- [23] S. Karlin and W. Studden. *Tchebycheff Systems with Applications in Analysis and Statistics*. Wiley-Interscience, 1966.
- [24] M. Lázaro-Gredilla, J. Quiñero-Candela, C. E. Rasmussen, and A. R. Figueiras-Vidal. Sparse spectrum gaussian process regression. *Journal of Machine Learning Research*, 11(63):1865–1881, 2010.
- [25] D. V. Lindley and A. F. M. Smith. Bayes estimates for the linear model. *Journal of the Royal Statistical Society. Series B (Methodological)*, 34(1):1–41, 1972.
- [26] R. Luger, D. Foreman-Mackey, and C. Hedges. Mapping stellar surfaces. ii. an interpretable gaussian process model for light curves. *The Astronomical Journal*, 162:124, Aug 2021.
- [27] J. Ma, V. Rokhlin, and S. Wandzura. Generalized gaussian quadrature rules for systems of arbitrary functions. *SIAM Journal on Numerical Analysis*, 33(3):971–996, 1996.
- [28] V. Minden, A. Damle, K. L. Ho, and L. Ying. Fast Spatial Gaussian Process Maximum Likelihood Estimation via Skeletonization Factorizations. *Multiscale Modeling and Simulation*, 15(4), 2017.
- [29] M. Munkhoeva, Y. Kapushev, E. Burnaev, and I. Oseledets. Quadrature-based features for kernel approximation. In S. Bengio, H. Wallach, H. Larochelle, K. Grauman, N. Cesa-Bianchi, and R. Garnett, editors, *Advances in Neural Information Processing Systems*, volume 31. Curran Associates, Inc., 2018.

- [30] T. Paananen, J. Piironen, M. R. Andersen, and A. Vehtari. Variable selection for gaussian processes via sensitivity analysis of the posterior predictive distribution. In *Proceedings of the Twenty-Second International Conference on Artificial Intelligence and Statistics*, volume 89, pages 1743–1752. PMLR, 16–18 Apr 2019.
- [31] J. Quinonero-Candela and C. E. Rasmussen. Analysis of some methods for reduced rank Gaussian process regression. In *Switching and learning in feedback systems*, pages 98–127. Springer, 2005.
- [32] A. Rahimi and B. Recht. Random features for large-scale kernel machines. In J. Platt, D. Koller, Y. Singer, and S. Roweis, editors, *Advances in Neural Information Processing Systems*, volume 20. Curran Associates, Inc., 2008.
- [33] C. E. Rasmussen and C. L. I. Williams. *Gaussian Processes for Machine Learning*. MIT Press, Cambridge, MA, 2006.
- [34] K. Serkh. *Personal correspondence*, 2021.
- [35] P. F. Shustin and H. Avron. Gauss-legendre features for gaussian process regression, 2021.
- [36] A. Solin and S. Särkkä. Hilbert space methods for reduced-rank Gaussian process regression. *Statistics and Computing*, 30, 2020.
- [37] M. L. Stein. *Interpolation of Spatial Data, Some Theory for Kriging*. Springer, New York, NY, 1999.
- [38] L. N. Trefethen. *Approximation Theory and Approximation Practice: Extended Edition*. SIAM, Philadelphia, PA, 2020.